

*Bioconiug Chem.* Author manuscript; available in PMC 2014 September 18.

Published in final edited form as:

Bioconjug Chem. 2013 September 18; 24(9): . doi:10.1021/bc400166j.

# Synthesis of polymer-lipid nanoparticles for image-guided delivery of dual modality therapy

Aneta J. Mieszawska<sup>a</sup>, YongTae Kim<sup>b</sup>, Anita Gianella<sup>a</sup>, Inge van Rooy<sup>a</sup>, Bram Priem<sup>a</sup>, Matthew P. Labarre<sup>c</sup>, Canturk Ozcan<sup>a</sup>, David P. Cormode<sup>d</sup>, Artiom Petrov<sup>e</sup>, Robert Langer<sup>b</sup>, Omid C. Farokhzad<sup>f</sup>, Zahi A. Fayad<sup>a</sup>, and Willem J. M. Mulder<sup>a,g</sup>

<sup>a</sup>Translational and Molecular Imaging Institute and Imaging Science Laboratories, Icahn School of Medicine at Mount Sinai, One Gustave L. Levy Place, New York, New York 10029, USA <sup>b</sup>David H. Koch Institute for Integrative Cancer Research, Department of Chemical Engineering and Division of Health Science and Technology, Massachusetts Institute of Technology, Cambridge, MA 02139, USA <sup>c</sup>Department of Materials Science and Engineering, University of Pennsylvania, 3451 Walnut Street, Philadelphia, PA 19104, USA <sup>d</sup>Radiology Department, University of Pennsylvania, 3400 Spruce Street, 1 Silverstein, Philadelphia, PA 19104, USA <sup>e</sup>Zena and Michael and Michael A. Wiener Cardiovascular Institute and Marie-Josée and Henry R. Kravis Center for Cardiovascular Health, Icahn School of Medicine at Mount Sinai, One Gustave L. Levy Place, New York, New York 10029, USA <sup>f</sup>Laboratory of Nanomedicine and Biomaterials, Department of Anesthesiology, Brigham & Women's Hospital, Harvard Medical School, 75 Francis Street, Boston, MA 02115, USA <sup>g</sup>Department of Vascular Medicine, Academic Medical Center, Amsterdam, The Netherlands

#### **Abstract**

For advanced treatment of diseases such as cancer, multi component, multi functional nanoparticles hold great promise. In the current study we report the synthesis of a complex nanoparticle (NP) system with dual drug loading as well as diagnostic properties. To that aim we present a methodology where chemically modified poly(lactic co glycolic) acid (PLGA) polymer is formulated into a polymer lipid NP that contains a cytotoxic drug doxorubicin (DOX) in the polymeric core and an anti angiogenic drug sorafenib (SRF) in the lipidic corona. The NP core also contains gold nanocrystals (AuNCs) for imaging purposes and cyclodextrin molecules to maximize the DOX encapsulation in the NP core. In addition, a near infrared (NIR) Cy7 dye was incorporated in the coating. To fabricate the NP we used a microfluidics based technique that offers unique NP synthesis conditions, which allowed for encapsulation and fine tuning of optimal ratios of all the NP components. NP phantoms could be visualized with computed tomography (CT) and near infrared (NIR) fluorescence imaging. We observed timed release of the encapsulated drugs, with fast release of the corona drug SRF and delayed release of a core drug DOX. In tumor bearing mice intravenously administered NPs were found to accumulate at the tumor site by fluorescence imaging.

## INTRODUCTION

Advances in nanotechnology in general, and nanoparticle (NP) production methods specifically, have facilitated and accelerated the development of complex multicomponent nanomaterials. In the past decade, a significant research effort by the nanomedicine community was focused on the development and preclinical application of NP platforms<sup>1-3</sup>. NP drug formulations can solubilize or shield hydrophobic or highly toxic cytostatic agents and overcome bioavailability challenges<sup>4-6</sup>. Also, NP systems can be used to alter pharmacokinetics and increase the percentage of injected drug dose that accumulates at the diseased site<sup>7-9</sup>. Finally, their favorable size range and the ease of surface functionalization enable targeting of NPs to specific cell types at these diseased sites<sup>10,11</sup>. However, the assembly of multiple materials and/or agents into one NP formulation is challenging and frequently necessitates extreme synthetic conditions that by themselves can impair functionality of the individual NP components.

In the current report, we present a highly complex and multifunctional hybrid polymer lipid NP platform that incorporates diagnostic nanocrystals and two therapeutic drugs. The complexity of the proposed NP required selecting a suitable synthesis method that would facilitate the integration of all functionalities into the NP, since other widely used NP synthesis techniques, including nanoprecipitation<sup>12</sup>, have failed at the incorporation of all necessary components into a NP. To this aim we used a two pronged approach that involved chemical modification of a polymer and the use of microfluidic technology, that we recently developed for high throughput polymer NP synthesis<sup>13</sup>. This microfluidic system provides a controlled mixing environment, which facilitates NP assembly through microvortices<sup>14</sup> at ambient conditions.

The NP core is composed of a biodegradable poly(lactic co glycolic acid) (PLGA) polymer, functionalized with gold nanocrystals (AuNCs), which serve as scaffolds that are loaded with doxorubicin (DOX), a widely used cytostatic agent<sup>15, 16</sup>. Since AuNCs are electron dense and exhibit good X ray attenuation properties the NP platform can be imaged by electron microscopy and computed tomography (CT)<sup>17, 18</sup>. The NP coating is comprised of ordinary phospholipids and PEGylated phospholipids at a 7/3 ratio, which by themselves form stable disks<sup>19</sup>. The latter facilitates the formation of a lipid monolayer around the PLGA core. This lipid coating provides biocompatibility, while PEG reduces clearance by the mononuclear phagocyte system (MPS) and thereby elongates circulation half lives<sup>20</sup>. We also used the lipidic coating to co encapsulate a second lipophilic drug sorafenib (SRF). SRF is an angiogenesis inhibitor with anti tumor activity<sup>21</sup>. Lastly, the PEG coating was labeled with Cy7 fluorophores for near infrared fluorescence (NIRF) imaging.

For cancer treatment the combination of administering an anti angiogenic and cytotoxic agent holds great promise to maximize the therapeutic outcome by interfering in the tumor blood/nutrients supply and simultaneously inducing cancer cell apoptosis<sup>22-24</sup>. However, an impaired vascular system also reduces the cytostatic agent influx into the tumor. NP systems accumulate at tumorous sites with a leaky vasculature through the enhanced permeability and retention effect (EPR)<sup>25</sup> and increase drug bioavailability and prolong the exposure to therapeutic agents providing slow release<sup>26</sup>. Dual drug loading in the NP systems with controlled release rates would potentially address the described limitations of the aforementioned combined drug therapy.

## **RESULTS AND DISCUSSION**

Previous PLGA DOX formulations have already been explored<sup>27, 28</sup>. Nevertheless, it remains challenging to incorporate high doses of DOX into the NP core. In order to

overcome this issue, we chemically modified PLGA using esterification reaction sequentially, as shown in Scheme 1. First, 1 3 nm AuNCs were conjugated to the PLGA polymer and subsequently these AuNCs were derivatized with hydroxypropyl cyclodextrin (HP CD), a cyclic drug host molecule<sup>29, 30</sup> that can be incorporated into polymeric NPs<sup>31</sup>. To that end the carboxyl groups of 11 mercaptoundecanoic acid (MUA) capped 3 nm AuNCs were reacted with hydroxyl groups of PLGA monomers using N,N dicyclohexylcarbodiimide (DCC) and 4 dimethylaminopyridine (DMAP), which resulted in the formation of an ester bond between the ligands of AuNCs and PLGA monomers. The same reaction conditions were used to attach HP CD to the AuNCs. To maximize loading of AuNCs and HP CD to the PLGA polymer, the esterification reaction can be repeated multiple times, to create AuNC:HP CD:AuNC:HP CD:etc chains. <sup>1</sup>H NMR was performed after each esterification step to confirm successful modification of the PLGA polymer (Figure S1, supporting information). From the <sup>1</sup>H NMR analyses it was found that there were 3.44 HP CD molecules per one PLGA monomer. In addition, the yield for each step of the PLGA modification was quantified. The Au concentration derived from CT measurements, for which detailed calculations are presented in the supporting information, was found to be 0.7 mg Au/100 mg of PLGA (89 % of the initial input value) and the concentration of HP CDs derived from NMR was established to be 12 mg HP CDs/100 mg PLGA (24 % of the initial input value).

The modified PLGA AuNCs HP CDs was incubated with DOX prior to NP synthesis to assure DOX HP CDs complex formation. The microfluidic chip for the rapid polymer lipid NP synthesis <sup>13</sup> is shown in (Figure 1A). PLGA modified with AuNCs HP CDs DOX in acetonitrile was infused in the center channel of a microfluidic chip. PEGylated phospholipids (PEG DSPE) and 1,2 dipalmitoyl sn glycero 3 phosphocholine (DPPC) in a 7:3 ratio were combined with SRF in 30 % methanol in water and infused in the external channels. 0.3 mol % of PEG DSPE labeled with the NIRF Cy7 dye was added to the lipids.

The polymer lipid NPs were assembled by dual microvortices created at the intersection of the three inlets of the microfluidic chip (Figure 1B) at a flow rate of 5 ml/min in the external channels and 1 ml/min in the center channel, which corresponded to a Reynolds number<sup>32</sup> of 150. These conditions provide controlled mixing environment on the microscale and facilitate the swift assembly of uniform NPs, as explained in details previously<sup>13</sup>. The DOX loading, established by HPLC, was 25.6% of the initial input value. This value is 19 times higher than DOX loading in polymer lipid NPs where PLGA was not modified with HP CDs (1.3% of the initial input value). Our strategy resulted in 2 (molar %) times higher DOX encapsulation in PLGA NPs as compared to a previously published method where DOX was directly conjugated to the PLGA polymer to elevate its encapsulation into the NP core and the NPs were formed using an emulsion solvent diffusion method<sup>28</sup>. The SRF encapsulation efficiency was established to be 66.0% of the initial input value.

The engineered polymer lipid NPs were thoroughly characterized with respect to efficiency of AuNCs encapsulation, size, and contrast generating properties, as depicted in Figure 2. Transmission electron microscopy (TEM) revealed the uniform incorporation of AuNCs in polymer lipid NPs (Figure 2A, enlarged image Figure S2). The NPs generated CT contrast, as shown in Figure 2B, and the CT attenuation rate<sup>33</sup> was 5.23 HU/mM as established previously<sup>34</sup>. The mean overall diameter of polymer lipid NPs was 85.1 nm with a polydyspersity of 0.1 as measured by dynamic light scattering (DLS) (Figure 2C). Importantly, due to the Cy7 incorporated in the lipid corona, the NPs produced strong fluorescence in the NIR region as shown in Figure 2D.

We tested the polymer lipid NPs for drug release under physiological conditions (in PBS at 37 °C), the results of which are shown in Figure 3. Drug concentrations were quantified

using HPLC (see supporting information for experimental details, figure S3 and S4). The SRF onset release was observed after 1 hour while DOX after 5 hours. The delayed release of DOX corroborates that the drug is incorporated in the polymeric core while the rapid release of SRF indicates its incorporation within the lipid corona of the NP. The rigidity of the lipidic coating, which has a phase transition temperature well above 37 °C, contributes to the partial preservation of SRF and its prolonged release. Both, SRF and DOX continued to release from the NPs for 21 days, classifying this nanoparticle as a 2<sup>nd</sup> generation sustained release platform.

To test biological activity human umbilical vein cells (HUVECs) and a human colon cancer cell line (LS174T) were incubated with NPs and cell viability was measured (Figure 4A). NPs containing both SRF and DOX reduced cell viability of HUVECs by 42% and the cell viability of LS174T cells by 72% as compared to the untreated control groups after 24 h of incubation. Cell viability was less affected by NPs containing a single drug, while the viability of cells incubated with NPs without a drug were similar to the untreated cells. We confirmed the results by live/dead staining (Figure 4B and C). After a 24 h incubation the number of dead cells was negligible for untreated cells as well as for cells treated with plain NP or NP containing AuNCs only. The number of dead cells increased for single drug NP formulations (see supporting Figure S5 for the control experiments). The concurrent presence of SRF and DOX in the NP formulation maximized the cytotoxic effects for both HUVECs and LS174T cells (Figure 4B C). The release profiles (fast SRF and delayed DOX release) combined with the in vitro finding suggest our NP platform may indeed find use as a NP that accumulates at the tumor site, acts on existing tumor blood vessels and prevents angiogenesis by SRF, followed by DOX induced cancer cell death. However, extensive mouse studies are required to establish the efficacy of our NPs in vivo in future studies.

However, we did perform pilot in vivo studies with tumor bearing mice to evaluate the NP tumor targeting potential. The NPs were intravenously administered into tumor bearing mice (n=3) and the animals were imaged 18 h post injection. Blood samples were collected at various time points. Optical measurements and fitting of the data revealed the in vivo half life of NPs to be 40 min. Anatomical CT imaging revealed the presence of a tumor on the flank of the animals. Figure 5A depicts a reconstructed 3D CT image of mouse topography; the arrow indicates the tumor site. Although the NPs contained gold tumor accumulation did not result in a detectable CT signal attenuation. Among the different imaging modalities CT is relatively insensitive to detecting exogenous agents. Although the AuNCs can also serve as a CT contrast agent<sup>8</sup>, the AuNCs in the presented lipid polymer NP primarily serve as inert scaffolds<sup>35, 36</sup> and their payload can potentially be increased as shown previously<sup>34</sup>, providing the option to use this NP platform as a CT imaging tool as well. However, NIRF imaging, a very sensitive imaging modality, revealed the accumulation of NPs in tumors (Figure 5B). Due to the limited imaging depth of NIRF imaging we also performed ex vivo NIRF of excised organs to more accurately establish NP biodistribution in relevant organs (supplementary Figure S6). Finally, to corroborate the accumulation of NPs we performed the immunofluorescence of tumor sections, depicted in Figure 6. Staining of endothelial cells (red) indicates tumor blood vessels. NPs (green) were found in close proximity of the vessels (Figure 6A) as well as in tumor interstitium (Figure 6B) indicative of NP extravasation and tumor accumulation. Ongoing studies are aimed to further optimize the NP's physicochemical properties as well as AuNCs payload per NP to enhance the NP tumor accumulation, and improve the in vivo NP detection by CT, respectively.

## CONCLUSION

In summary, we combined simple carbodiimide conjugation chemistry to modify the PLGA polymer to synthesize a complex and multifunctional theranostic polymer lipid NP platform

with microfluidic technology. Two drugs, i.e. the anti angiogenic drug SRF and cytotoxic drug DOX, for combined cancer therapy were successfully encapsulated in the lipid corona and polymeric core, respectively. Release profiles showed a quick release of SRF and a delayed release of DOX. Finally, an in vivo pilot NIRF imaging experiment revealed the accumulation of the NPs at the tumor site and immuno fluorescence of tumor sections revealed distribution of the NPs within the tumor space. Future studies are planned to evaluate the efficacy of our approach in vivo in tumor bearing mice. In addition to cancer therapy the flexibility of our NP platform allows for incorporation of other therapeutics and applications of a theranostic NP probe for atherosclerotic disease or other pathologies that are characterized by ongoing angiogenesis.

#### **EXPERIMENTAL SECTION**

#### **Materials**

1 dodecanethiol, 11 mercaptoundecanoic acid, 4 dimethylaminopyridine, N,N - dicyclohexylurea, Poly(D,L lactide co glycolide) lactide:glycolide (50:50), mol wt 30,000 60,000, chloroauric acid, sodium borohydride, methyl trioctylammonium chloride, cis 9 octadecene 1 thiol, (2 Hydroxypropyl) cyclodextrin, and doxorubicin hydrochloride were purchased from Sigma Aldrich (St. Louis, MO). 1,2 distearoyl sn glycero 3 phosphoethanolamine N [methoxy(polyethylene glycol) 2000] (PEG2000 DSPE) and 1,2 dipalmitoyl *sn* glycero 3 phosphocholine (DPPC) were purchased from Avanti Polar Lipids, Inc. (Alabaster, AL). Sorafenib p toluenesulfonate salt was purchased from Biotang Inc (Lexington, MA).

## Synthesis of Au nanocrystals (AuNCs)

AuNCs coated with 1 dodecanethiol were prepared using a previously published method by Brust et al.<sup>37</sup> The AuNCs were 1 3 nm in diameter and the hydrophobic nature of the capping ligands rendered them soluble in organic solvents such as toluene and chloroform.

## AuNCs ligand exchange

Hydrophobic dodecanethiol ligands on AuNCs (108 ligands per one AuNC) were exchanged to mercaptoundecanoic acid (MUA) following the Murray method<sup>38</sup>. 100 mg of dodecanethiol capped AuNCs were dissolved in 20 ml of toluene and mixed with 70 mg of MUA (at a 1:5 molar ratio of dodecanethiol:MUA) and stirred for 96 hrs. Next, toluene was removed by evaporation using a rotary evaporator with a 70 °C water bath. The AuNCs were resuspended and washed with acetonitrile (ACN) and collected on a frit (Opti Chem). The ligand exchange reaction renders the AuNCs MUA soluble in polar solvents i.e. ethanol (EtOH), methanol (MeOH) or dimethylformamide (DMF).

## PLGA modification with AuNCs and (2 Hydroxypropyl) $\beta$ cyclodextrin (HP $\beta$ CD)

100 mg of PLGA (average MW of 60,000 g/mol) and 3 mg of AuNCs MUA (centrifuged at 14.5K rpm to remove precipitated AuNCs) were dissolved in 1 ml of DMF. The esterification reaction between the alcohol group of PLGA and the carboxylic acid group of MUA was performed using the coupling reagent N,N' dicyclohexylurea (DCC), and the base 4 dimethylaminopyridine (DMAP), which were added at 20 mM concentration (both). After 3 hours of gentle stirring, DMF was evaporated and PLGA AuNC conjugates were dissolved in ACN at a concentration of 20 mg/ml and stored overnight in 20°C freezer to precipitate unreacted AuNCs. The supernatant was used in further steps. Next, the PLGA AuNCs were transferred to 1 ml DMF, mixed with 50 mg of HP CD (5 × molar excess with respect to PLGA) and 20 mM DCC and DMAP and stirred for 3 hrs. After 3 hrs DMF was evaporated and PLGA AuNCs HP CD dissolved in ACN at a concentration of 20 mg/ml of

PLGA, stored in 20  $^{\circ}$ C freezer overnight to precipitate unreacted HP CD. The supernatant was used in subsequent steps. The coupling of AuNCs to PLGA AuNCs HP CD was repeated. The final PLGA AuNCs HP CD AuNCs solution in ACN was clear and tinted brownish/red. Small fraction of the PLGA polymer was modified with Cy5.5 using the same conjugation chemistry.

#### Formation of lipid polymer NPs using microfluidics

Lipid polymer NPs were formed using a microfluidic method developed by Kim et al. <sup>13</sup>. In short, 250 μg of doxorubicin was dissolved in DMF and mixed with 12 mg of PLGA AuNCs HP CD AuNCs in ACN at 2 mg/ml final PLGA concentration. 250 μg of sorafenib (SRF) was mixed with 59.5 ml of DPPC/DSPE PEG (molar ratio of 3:7 of DPPC:DSPE PEG and 0.3 molar % of DSPE PEG Cy7) in 30% MeOH/H<sub>2</sub>O at 0.04 mg/ml of total lipids. The PLGA AuNCs HP CD DOX AuNCs solution was infused in the middle channel at 1 ml/min and lipids SRF solution in the external channels at 5ml/min. The formed lipid polymer NP solution was stirred overnight under the fume hood to evaporate the solvents, subsequently filtered through a 0.22 μm syringe filter to remove the residual DCC and washed extensively with water using Vivaflow® 50 filtration system (Sartorius, Bohemia, NY) to remove residual DMAP and unbound DOX/SRF. The NPs used in fluorescent imaging of tumor sections contained 7 mol % of PLGA labeled with Cy5.5.

#### In vitro drug release experiments

The NPs were washed thoroughly with purified water after the synthesis and preconcentrated using a Vivaflow® 50 filtration system (Sartorius, Bohemia, NY). 500  $\mu$ L of NP samples, corresponding to 4 mg of PLGA each, were placed in dialysis cassettes with a 2 kDa MWCO membrane (Pierce, Rockford, IL). At each timepoint three NP samples were collected, dried under vacuum and the drugs were resolubilized in 500  $\mu$ L of methanol. The samples were then centrifuged at 14.5K rpm for 5 min to remove the polymer and the supernatant was collected. The samples were analyzed for SRF and DOX content using HPLC as described in supplementary section.

#### **Tumor mouse model**

To establish subcutaneous tumors 4 female nude mice were inoculated with  $2\times10^6$  LS174T cells on the right flank. After 4 days the tumors were palpable and at 9 days tumor volumes reached 100 - 120 mm³. NPs corresponding to 240 mg of PLGA and labeled with the near infrared dye Cy7 were administrated trough tail vein injection to 3 mice. One mouse was not injected and was used as a control. Eighteen hours post injection, mice were anesthetized using ketamine/xylamine mixture (100mg/kg / 10mg/kg) to enable in vivo CT and near infrared fluoresce (NIRF) imaging. After in vivo imaging mice were sacrificed and the organs collected for NIRF imaging of NP biodistribution. For the in vivo half life the blood samples were drawn from the lateral saphenous vein at 5, 10, 60, and 120 min.

#### **Immunofluorescence**

Frozen tumor sections were prepared using a cryostat. Standard immunostaining techniques were appled for CD31 and dapi. In short, the sections were blocked with donkey serum for 20 min, washed with PBS and incubated with rat anti mouse CD31 antibody (BD Pharmigen #553370) for 45 min. The slides were rinsed with PBS and incubated with secondary donkey anti rat antibody (Jackson Immuno Research Laboratories, Inc. #712 165 150) labeled with Cy3 for 30 min, rinsed with PBS and mounted in mounting medium with DAPI (Vector laboratories, Burlingame CA). The stained tumor sections were imaged using Leica Microsystems DM6000 microscope controlled using Leica Application Suite Advanced

Fluorescence (LAS AF) software version 3.1.0 build 8587. The microscope was fitted with a Leica DFC350 FX camera. Sections were imaged at 40 and 63 times magnification.

# **Supplementary Material**

Refer to Web version on PubMed Central for supplementary material.

## **Acknowledgments**

This work was supported by the National Heart, Lung, and Blood Institute, National Institutes of Health, as a Program of Excellence in Nanotechnology (PEN) Award, Contract #HHSN268201000045C, as well as by R01 EB009638 (Z.A.F.), R00 EB012165 (D.P.C.) and R01 CA155432 (W.J.M.M.).

#### References

- (1). Peer D, Karp JM, Hong S, Farokhzad OC, Margalit R, Langer R. Nanocarriers as an emerging platform for cancer therapy. Nat Nanotechnol. 2007; 2:751–60. [PubMed: 18654426]
- (2). Torchilin VP. Recent advances with liposomes as pharmaceutical carriers. Nat Rev Drug Discov. 2005; 4:145–60. [PubMed: 15688077]
- (3). Wagner V, Dullaart A, Bock AK, Zweck A. The emerging nanomedicine landscape. Nat Biotechnol. 2006; 24:1211–7. [PubMed: 17033654]
- (4). Dalwadi G, Sunderland B. An ion pairing approach to increase the loading of hydrophilic and lipophilic drugs into PEGylated PLGA nanoparticles. Eur J Pharm Biopharm. 2009; 71:231–42. [PubMed: 18768159]
- (5). Wischke C, Schwendeman SP. Principles of encapsulating hydrophobic drugs in PLA/PLGA microparticles. Int J Pharm. 2008; 364:298–327. [PubMed: 18621492]
- (6). Zhang L, Chan JM, Gu FX, Rhee JW, Wang AZ, Radovic Moreno AF, Alexis F, Langer R, Farokhzad OC. Self assembled lipid polymer hybrid nanoparticles: a robust drug delivery platform. ACS Nano. 2008; 2:1696–702. [PubMed: 19206374]
- (7). Avgoustakis K, Beletsi A, Panagi Z, Klepetsanis P, Karydas AG, Ithakissios DS. PLGA mPEG nanoparticles of cisplatin: in vitro nanoparticle degradation, in vitro drug release and in vivo drug residence in blood properties. J Control Release. 2002; 79:123–35. [PubMed: 11853924]
- (8). Cormode DP, Roessl E, Thran A, Skajaa T, Gordon RE, Schlomka JP, Fuster V, Fisher EA, Mulder WJ, Proksa R, Fayad ZA. Atherosclerotic plaque composition: analysis with multicolor CT and targeted gold nanoparticles. Radiology. 2010; 256:774–82. [PubMed: 20668118]
- (9). Gianella A, Jarzyna PA, Mani V, Ramachandran S, Calcagno C, Tang J, Kann B, Dijk WJ, Thijssen VL, Griffioen AW, Storm G, Fayad ZA, Mulder WJ. Multifunctional nanoemulsion platform for imaging guided therapy evaluated in experimental cancer. ACS Nano. 2011; 5:4422–33. [PubMed: 21557611]
- (10). Hrkach J, Von Hoff D, Mukkaram Ali M, Andrianova E, Auer J, Campbell T, De Witt D, Figa M, Figueiredo M, Horhota A, Low S, McDonnell K, Peeke E, Retnarajan B, Sabnis A, Schnipper E, Song JJ, Song YH, Summa J, Tompsett D, Troiano G, Van Geen Hoven T, Wright J, LoRusso P, Kantoff PW, Bander NH, Sweeney C, Farokhzad OC, Langer R, Zale S. Preclinical development and clinical translation of a PSMA-targeted docetaxel nanoparticle with a differentiated pharmacological profile. Sci Transl Med. 2012; 4:128ra39.
- (11). Sengupta S, Eavarone D, Capila I, Zhao G, Watson N, Kiziltepe T, Sasisekharan R. Temporal targeting of tumour cells and neovasculature with a nanoscale delivery system. Nature. 2005; 436:568–72. [PubMed: 16049491]
- (12). Xiong S, Zhao X, Heng BC, Ng KW, Loo JS. Cellular uptake of Poly (D,L lactide co glycolide) (PLGA) nanoparticles synthesized through solvent emulsion evaporation and nanoprecipitation method. Biotechnol J. 2011; 6:501–8. [PubMed: 21259442]
- (13). Kim Y, Lee Chung B, Ma M, Mulder WJ, Fayad ZA, Farokhzad OC, Langer R. Mass production and size control of lipid polymer hybrid nanoparticles through controlled microvortices. Nano Lett. 2012; 12:3587–91. [PubMed: 22716029]

(14). Marre S, Jensen KF. Synthesis of micro and nanostructures in microfluidic systems. Chem Soc Rev. 2010; 39:1183–202. [PubMed: 20179831]

- (15). Duyndam MC, van Berkel MP, Dorsman JC, Rockx DA, Pinedo HM, Boven E. Cisplatin and doxorubicin repress Vascular Endothelial Growth Factor expression and differentially down regulate Hypoxia inducible Factor I activity in human ovarian cancer cells. Biochem Pharmacol. 2007; 74:191–201. [PubMed: 17498666]
- (16). Fornari FA, Randolph JK, Yalowich JC, Ritke MK, Gewirtz DA. Interference by doxorubicin with DNA unwinding in MCF 7 breast tumor cells. Mol Pharmacol. 1994; 45:649–56. [PubMed: 8183243]
- (17). Hainfeld JF, Slatkin DN, Focella TM, Smilowitz, H M. Gold nanoparticles: a new X ray contrast agent. Br J Radiol. 2006; 79:248–53. [PubMed: 16498039]
- (18). Xu C, Tung GA, Sun S. Size and Concentration Effect of Gold Nanoparticles on X ray Attenuation As Measured on Computed Tomography. Chem Mater. 2008; 20:4167–4169. [PubMed: 19079760]
- (19). Johnsson M, Edwards K. Liposomes, disks, and spherical micelles: aggregate structure in mixtures of gel phase phosphatidylcholines and poly(ethylene glycol) phospholipids. Biophys J. 2003; 85:3839–47. [PubMed: 14645073]
- (20). Gref R, Minamitake Y, Peracchia MT, Trubetskoy V, Torchilin V, Langer R. Biodegradable long circulating polymeric nanospheres. Science. 1994; 263:1600–3. [PubMed: 8128245]
- (21). Wilhelm SM, Adnane L, Newell P, Villanueva A, Llovet JM, Lynch M. Preclinical overview of sorafenib, a multikinase inhibitor that targets both Raf and VEGF and PDGF receptor tyrosine kinase signaling. Mol Cancer Ther. 2008; 7:3129–40. [PubMed: 18852116]
- (22). Kerbel RS, Kamen BA. The anti angiogenic basis of metronomic chemotherapy. Nat Rev Cancer. 2004; 4:423–36. [PubMed: 15170445]
- (23). Ma J, Waxman DJ. Combination of antiangiogenesis with chemotherapy for more effective cancer treatment. Mol Cancer Ther. 2008; 7:3670–84. [PubMed: 19074844]
- (24). Teoh D, Secord AA. Antiangiogenic agents in combination with chemotherapy for the treatment of epithelial ovarian cancer. Int J Gynecol Cancer. 2012; 22:348–59. [PubMed: 22266932]
- (25). Iyer AK, Khaled G, Fang J, Maeda H. Exploiting the enhanced permeability and retention effect for tumor targeting. Drug Discov Today. 2006; 11:812–8. [PubMed: 16935749]
- (26). Mattheolabakis G, Rigas B, Constantinides PP. Nanodelivery strategies in cancer chemotherapy: biological rationale and pharmaceutical perspectives. Nanomedicine. 2012; 7:1577–90. [PubMed: 23148540]
- (27). Jia Y, Yuan M, Yuan H, Huang X, Sui X, Cui X, Tang F, Peng J, Chen J, Lu S, Xu W, Zhang L, Guo Q. Co encapsulation of magnetic Fe3O4 nanoparticles and doxorubicin into biodegradable PLGA nanocarriers for intratumoral drug delivery. Int J Nanomedicine. 2012; 7:1697–708. [PubMed: 22619520]
- (28). Yoo HS, Oh JE, Lee KH, Park TG. Biodegradable nanoparticles containing doxorubicin PLGA conjugate for sustained release. Pharm Res. 1999; 16:1114–8. [PubMed: 10450940]
- (29). Stella VJ, Rajewski RA. Cyclodextrins: their future in drug formulation and delivery. Pharm Res. 1997; 14:556–67. [PubMed: 9165524]
- (30). Uekama K, Hirayama F, Irie T. Cyclodextrin Drug Carrier Systems. Chem Rev. 1998; 98:2045–2076. [PubMed: 11848959]
- (31). Tao HQ, Meng Q, Li MH, Yu H, Liu MF, Du D, Sun SL, Yang HC, Wang YM, Ye W, Yang LZ, Zhu DL, Jiang CL, Peng HS. HP beta CD PLGA nanoparticles improve the penetration and bioavailability of puerarin and enhance the therapeutic effects on brain ischemia reperfusion injury in rats. Naunyn Schmiedebergs Arch Pharmacol. 2013; 386:61–70. [PubMed: 23192284]
- (32). Nguyen NT, Wu Z. Micromixers a review. J. Micromech. Microeng. 2005; 15:R1.
- (33). Galper MW, Saung MT, Fuster V, Roessl E, Thran A, Proksa R, Fayad ZA, Cormode DP. Effect of computed tomography scanning parameters on gold nanoparticle and iodine contrast. Invest Radiol. 2012; 47:475–81. [PubMed: 22766909]
- (34). Mieszawska AJ, Gianella A, Cormode DP, Zhao Y, Meijerink A, Langer R, Farokhzad OC, Fayad ZA, Mulder WJ. Engineering of lipid coated PLGA nanoparticles with a tunable payload of diagnostically active nanocrystals for medical imaging. Chem Commun. 2012; 48:5835–7.

(35). McMahon KM, Mutharasan RK, Tripathy S, Veliceasa D, Bobeica M, Shumaker DK, Luthi AJ, Helfand BT, Ardehali H, Mirkin CA, Volpert O, Thaxton CS. Biomimetic high density lipoprotein nanoparticles for nucleic acid delivery. Nano Lett. 2011; 11:1208–14. [PubMed: 21319839]

- (36). Zheng D, Giljohann DA, Chen DL, Massich MD, Wang XQ, Iordanov H, Mirkin CA, Paller AS. Topical delivery of siRNA based spherical nucleic acid nanoparticle conjugates for gene regulation. Proc Natl Acad Sci U S A. 2012; 109:11975–80. [PubMed: 22773805]
- (37). Brust M, Walker M, Bethell D, Schiffrin DJ, Whyman R. Synthesis of thiol derivatised gold nanoparticles in a two phase Liquid Liquid system. J. Chem. Soc., Chem. Commun. 1994; 7:801–802.
- (38). Guo R, Song Y, Wang G, Murray RW. Does core size matter in the kinetics of ligand exchanges of monolayer protected Au clusters? J Am Chem Soc. 2005; 127:2752–7. [PubMed: 15725033]

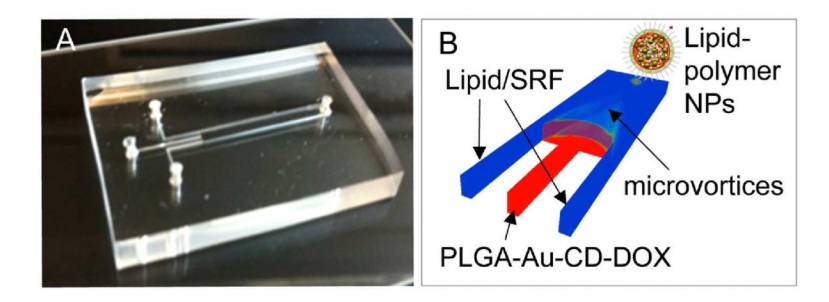


Figure 1.
(A) Microfluidic chip and (B) schematic of the flow pattern in the microfluidic chip.

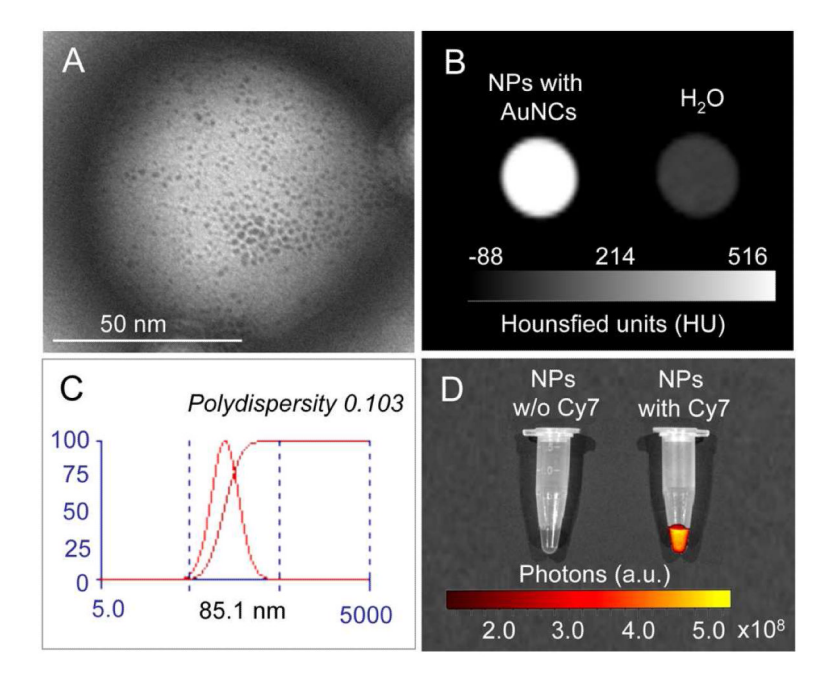
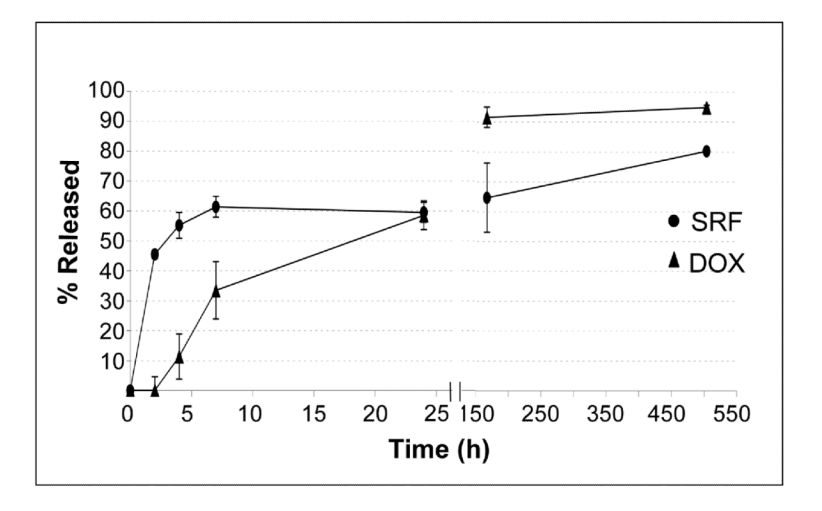
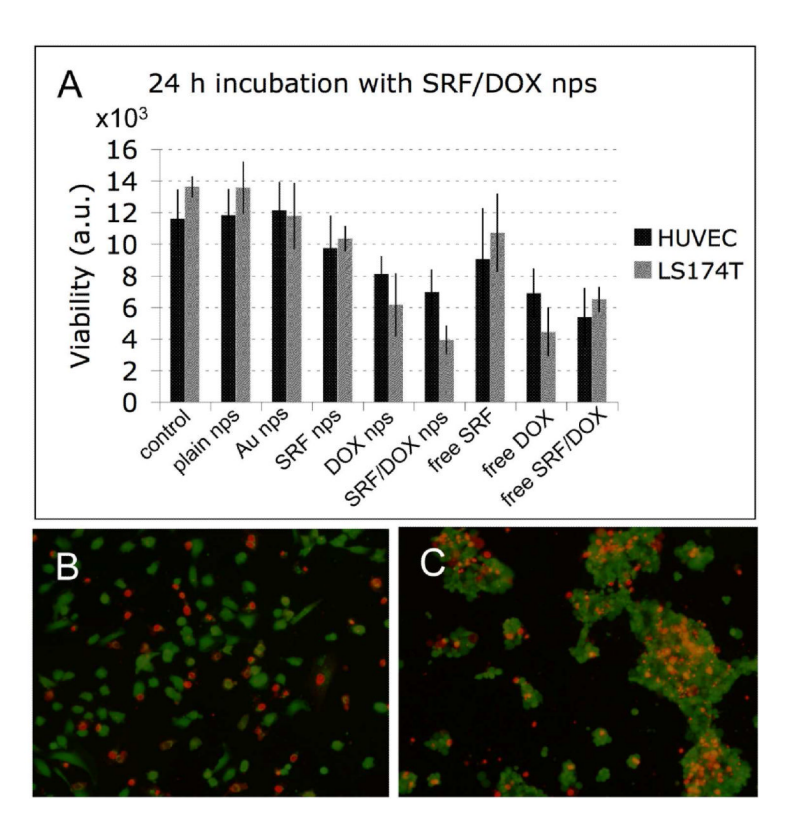


Figure 2.

(A) TEM image of a single engineered lipid polymer NP revealing encapsulated AuNCs; (B) CT image of phantoms containing AuNC loaded lipid polymer NPs or water; (C) DLS measurements of the NP platform; (D) fluorescence from Cy7 dye conjugated to NP's lipid corona.



**Figure 3.** Release profiles of SRF and DOX from NPs in PBS at 37°C



**Figure 4.** In vitro viability assays after incubating HUVEC and LS174T cells for 24 h with lipid polymer NPs containing SRF and DOX. (A) Luminescent cell viability assay; (B) Live (green)/dead (red) staining of HUVEC; (C) Live/dead staining of LS 174T cells.

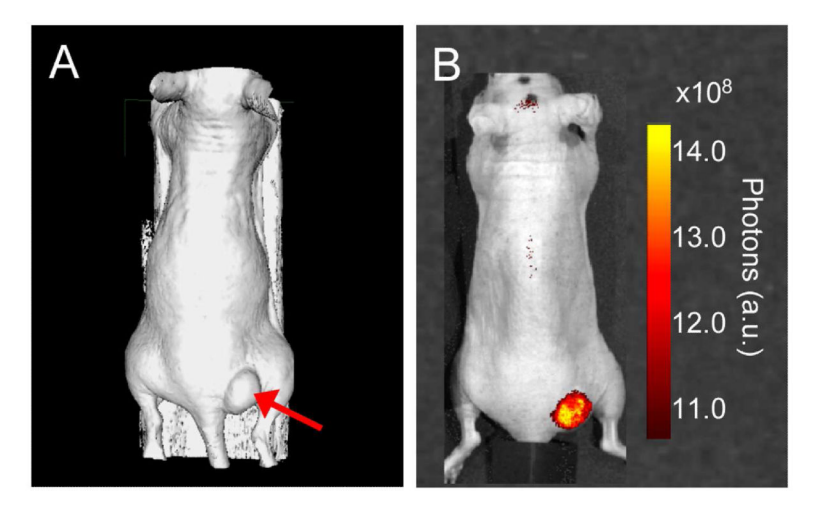


**Figure 5.** In vivo imaging of NPs biodistribution. (A) Reconstructed CT image of a tumor bearing mouse (arrow indicates the tumor), (B) NIRF imaging of strong Cy7 fluorescence in the tumor, indicative of NP accumulation.

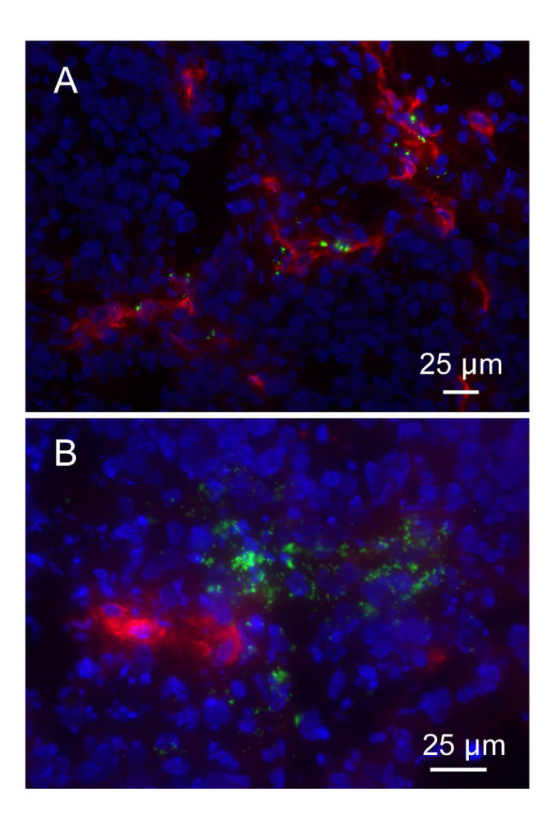
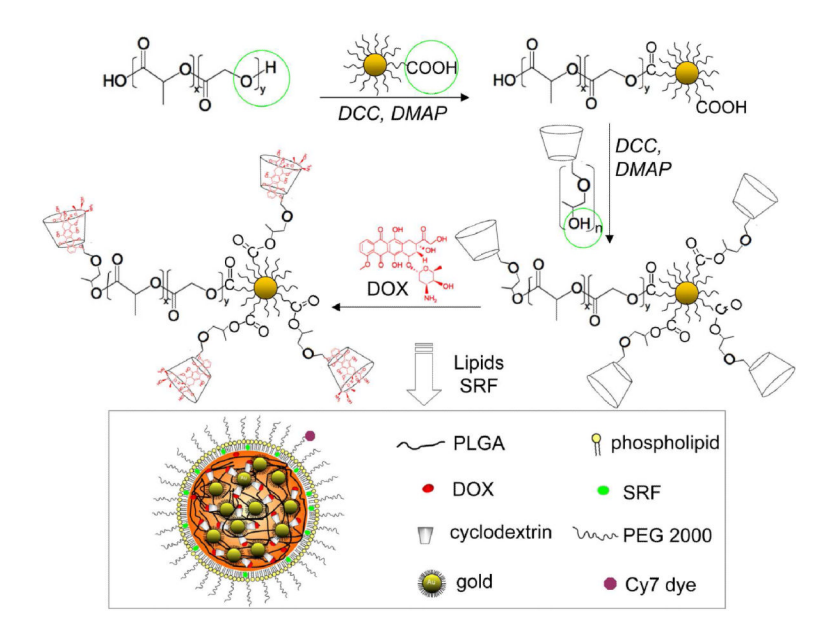


Figure 6. Immunofluorescence of tumor sections. CD31 staining shows endothelial cells in red, the NPs are shown in green and the nuclei are stained with dapi in blue. (A) The NPs were found associated with tumor blood vessels as well as (B) accumulated in the tumor interstitium.



**Scheme 1.** Modification of a PLGA polymer with AuNCs and HP CDs via an esterification reaction and subsequent host guest inclusion of DOX in HP CDs. Boxed: Lipid polymer NP formed from modified PLGA, lipids and SRF.